[논 문] 한국재료학회지
Korean Journal of Materials Research
Vol. 8, No. 2 (1998)

Levitation force of melt-textured single- and multi-domain YBaCuO superconductors

Yi-Sung Lee, Hyun-Soon Park, Il-Hyun Kuk*, Gye-Won Hong* and Chan-Joong Kim*

Department of Metallurgical Engineering, Sungkyunkwan University, Soowon, Kyounggi-do, 440-756, Korea
**Superconductivity Research Laboratory, Korea Atomic Energy Research Institute, P. O. Box 105, Yusung, Taejon, 305-600, Korea*

용융법으로 제조한 단결정형과 다결정형 YBaCuO 초전도체의 부상력

이이성 · 박현순 · 국일현* · 홍계원* · 김찬중*

성균관대학교 금속공학과
*한국원자력연구소 기능성재료연구팀

(1997년 10월 24일 받음, 1997년 12월 4일 최종수정본 받음.)

초 록 용융집합조직 YBaCuO 초전도체의 부상력에 미치는 변수들에 대하여 연구하였다. 초전도체의 부상력은 초전도체를 냉각하는 방법, 초전도결정의 방위, 시편의 두께 및 영구자석의 극성변화에 따라 달라짐을 알 수 있었다. 무자력 냉각한 초전도체에서는 큰 부상력과 작은 인력성분이 얻어지는 반면, 자력냉각한 시료에서는 반대의 결과가 얻어졌다. 이는 초전도체내에 포획된 자력양이 서로 다르고, 이들의 외부자장에 대한 상호작용이 다르기 때문인 것으로 판단된다. 초전도체의 부상력은 외부자력의 방향이 초전도결정의 c축과 평행할 경우(H//c-axis)가 c-축과 수직한 경우(H//ab-axis)보다 부상력이 2-3배 컸다. 표면자력 3500 gauss의 영구자석을 사용할 경우 초전도체의 두께가 약 8 mm 이상에서 초전도체의 부상력은 거의 일정하나 그 이하의 두께에서는 두께감소에 따라 선형적으로 감소하였다.

Abstract Parameters affecting the magnetic levitation force of the melt-textured YBCO superconductors were studied. The levitation force was dependent on the cooling method, the crystal orientation and the sample thickness of the superconductors and the polarity of the used permanent magnet. (i) the force-distance curves showed a hysteresis behavior depending on the cooling method of the superconductors (field cooling(FC) and zero field cooling(ZFC)), which is due to the different amounts of the magnetic fields trapped in the samples and the interaction to an external field, (ii) the repulsive force single domain sample grown to the c-axis (H//c-axis) is much larger than that of the sample grown to the a-b direction(H//ab-axis), (iii) the repulsive and the attractive force of the single domain sample have thickness dependence. It increases with increasing sample thickness and then reaches the saturation point.

1. Introduction

The origin of the levitation force of the oxide superconductor at the condition that an external magnetic field is lower than H_{c1} is the Meissner effect due to the perfect rejection of the magnetic field. In the case that the external magnetic fields are in the range between H_{c1} and H_{c2}, i. e., a mixed state of superconducting and normal states, the external magnetic field penetrates the superconductor and some of the field is trapped in the superconductor. The levitation force of the mixed state is mainly due to the magnetic field trapped in the superconductor and is much larger than that due to the Meissner effect[1,2]. Particularly, the melt-processed YBCO superconductors show very large levitation and the attractive forces due to the strong flux pinning capacity of the superconducting phase and the large grain[3]. The large levitation force makes it possible to use this material to the levitation applications such as contactless bearings[4~6], a high-speed motor[5,7], a flywheel energy storage[8~10] and levitation transportation systems[11] utilizing the interaction between a permanent magnet and the superconductors. The levitation force of a superconductor are expressed by the following equations[3],

$$F = m(dH/dx) \quad (1)$$

$$m = MV \quad (2)$$

$$M = AJ_c r \quad (3)$$

where m is a magnetic moment of a superconductor, dH/dx is a field gradient produced by the external field, M is a magnetization per unit volume, A is a constant depending on a sample geometry, J_c is a critical current density of a superconductor and r is the radius of the shielding current loop. This equation indicates that the

levitation force depends on factors such as grain size, phase purity, flux pinning and critical current density of the superconductor and the magnetic field of a permanent magnet. Since M is a function of J_c and r, therefore, the large levitation force can be achieved in the superconductors with strong flux pinning capability and a large grain. In addition, J_c depends on the crystal orientation[12], the defect density of the oxide superconductors[13,14] and the direction of the external field. For the practical applications of the YBCO superconductor, therefore, the material factors should be optimized to have the maximum levitation force, with an understanding of the interaction between the superconductor and a permanent magnet.

On the other hand, the properties of a permanent magnet such as magnetic strength, the field uniformity and the size of the magnet influence the levitation force[15]. For example, the levitation force increases with increasing magnetic strength of a permanent magnet[15]. It also a function of the size of a permanent magnet. The levitation force becomes a maximum value when the size of the used magnet is the same as the dimension of the superconducting sample. Furthermore, the uniformity of the magnetic field of a permanent magnetic is important particularly for the rotating device such as the flywheel energy storage system and the non-contact bearings, because the speed and the efficiency of the rotor are a function of the uniformity of the magnetic field[16]. We studied the interaction between melt-textured YBCO superconductor and the magnetic levitation force at 77K. The levitation forces of the melt-textured YBCO samples were systematically investigated with variables of a cooling method, a crystal orientation, a sample thickness of the superconductors, a polarity of the used permanent magnet.

2. Experiments

2. 1. Sample preparation

The samples used in this experiment is a melt-textured single- and multi-domain $YBa_2Cu_3O_{7-x}$ (Y123) containing Y_2BaCuO_5 (Y211) inclusions, prepared from a mixture of 1 mole of the calcined Y123 powder and 0.4 mole of Y211 powder. Raw powders of Y_2O_3, $BaCO_3$ and CuO of 99.9% purity were weighed to the cation ratio of Y : Ba : Cu = 1.8 : 2.4 : 3.4 and then mixed for 24 h in alcohol by ball milling, with 1 wt.% CeO_2 addition in order to refine the Y211 inclusion during melt processing[16]. The mixture powder was dried in air and calcined in air for 40 h in Al_2O_3 crucibles, with repeated crushing for every 10 h calcination. 90 g of the calcined powder was uniaxially pressed into pellets in a steel mold with a diameter of 40 mm and isostatically pressed again. The pellets were placed on MgO single crystal substrates and then melt-texturing heat treatment was followed. The detail of the melt texturing

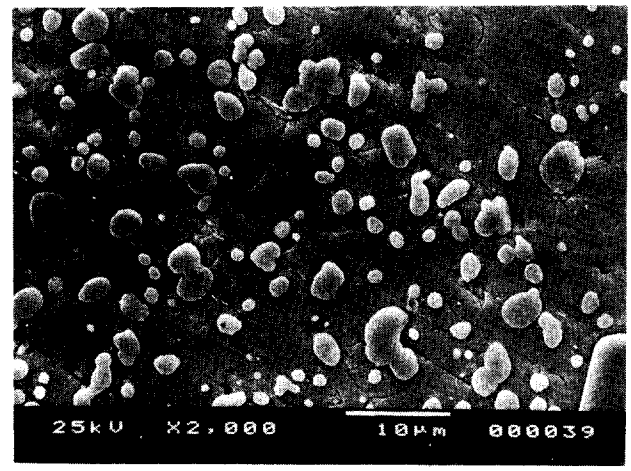

Fig. 1. Scanning electron micrograph of melt-textured YBCO showing fine Y211 particles trapped within the Y123 matrix.

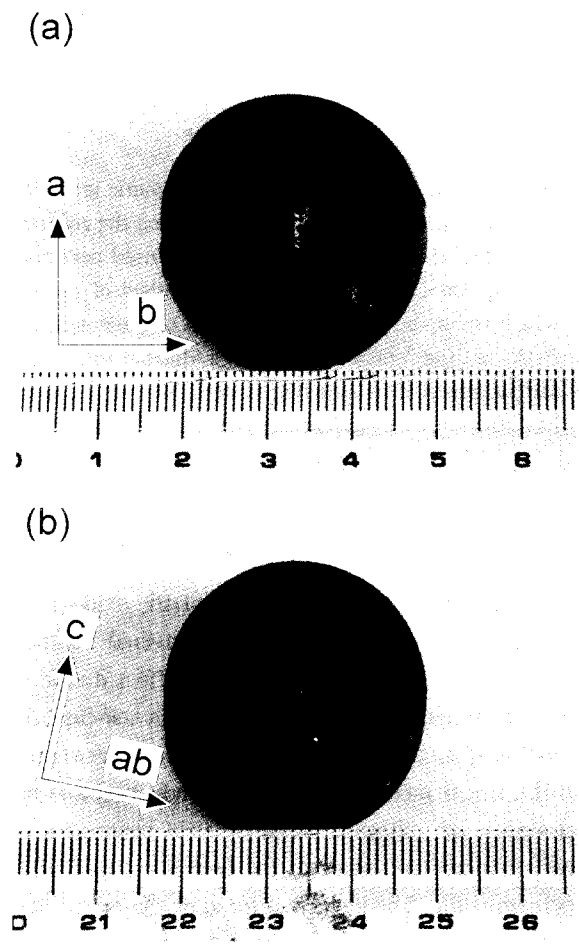

Fig. 2. Photos of the YBCO samples grown to (a) ab-axis and (b) c-axis.

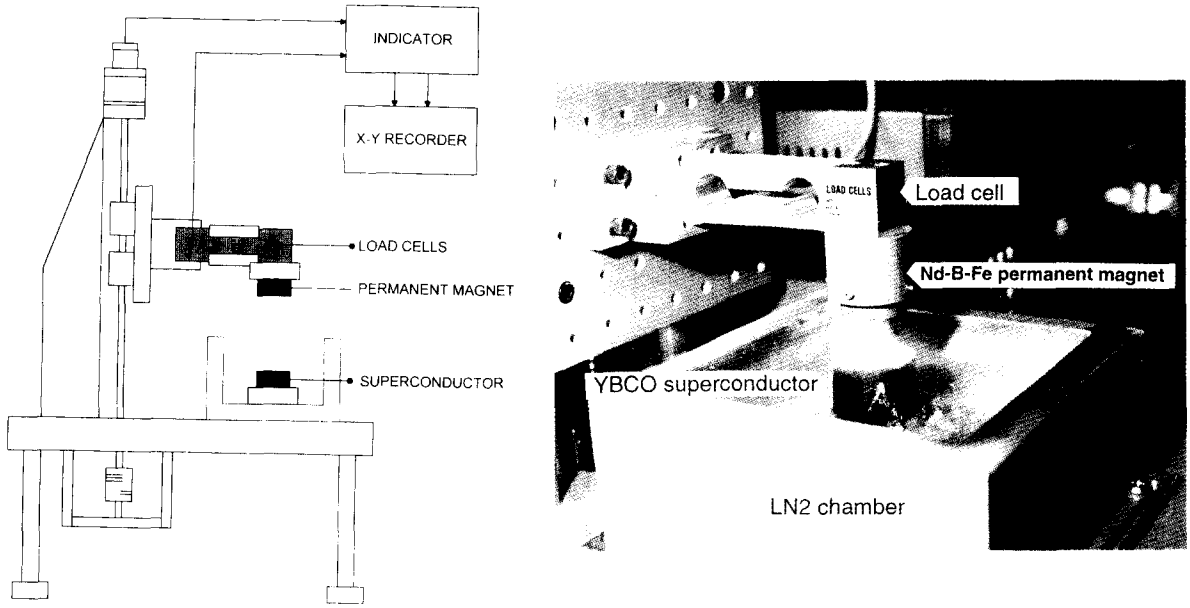

Fig. 3. Levitation measurement system

process was reported elsewhere[17]. The final dimension of the melt-textured samples was 33 mm (diameter) × 25 mm (thickness). Figure 1 shows scanning electron micrograph of the melt-textured YBCO sample. It can be seen that many Y211 particles are finely dispersed in the textured Y123 matrix, with a size distribution of 2 to 5 microns. The size of the grown Y123 domains was 1-2 cm.

Single-domain YBCO samples were grown normal and parallel to the c-axis of Y123 by the top-seeded melt-texturing technique with undercooling. The $NdBa_2Cu_3O_{7-\delta}$ (Nd123) crystals were used as a seed for the seeded melt texturing processing. The sintered YBCO samples were heated to 1100 ℃ for 1 h and then cooled to 1020 ℃ with a cooling rate of 100 ℃. At 1020 ℃, the Nd123 crystal was placed on the top of the YBCO samples, undercooled to 990 ℃ at a rate of 1 ℃/h were maintained at this temperature for 200 h and then cooled to room temperature. The samples were oxygenated in flowing oxygen for 50-100 h. Figure 2 shows photo of the seeded melt-textured YBCO sample grown to (a) ab-axis and (b) c-axis. The size of the grown Y123 domain was as large as 3 cm.

2. 2. Levitation force measurement

In order to estimate the repulsive and the attractive force between melt-textured YBCO samples, we designed a levitation force measurement system shown in Fig. 3. A disc-shaped Nd-B-Fe permanent magnet was placed below the cantilever beam where a load cell

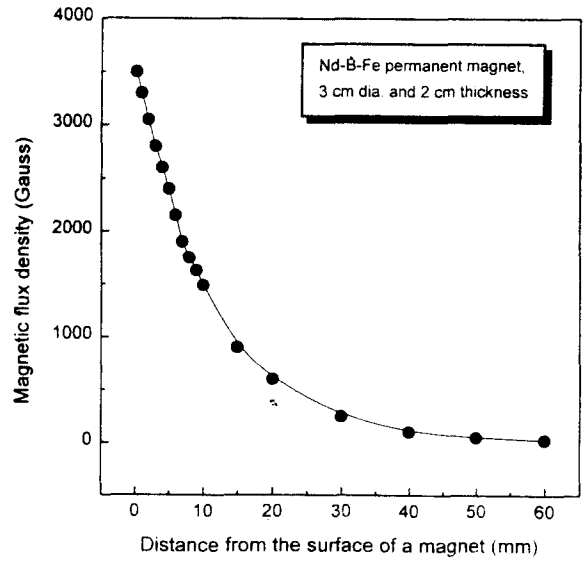

Fig. 4. Variation of magnetic flux density as a function of distance.

of which capacity is 30kgf was attached. Moving the permanent magnet toward and away from the sample cooled to 77K in a liquid nitrogen bath, force-distance curves were obtained. The dimension of the used magnet was 30 mm (diameter) × 20 mm (thickness). The surface magnetic flux density was 3500 Gauss (G) and the density at 10 mm distance was 1500 G (see Fig. 4).

Variation of a cooling method of a superconductor may lead to a different interaction between the YBCO superconductor and a permanent. For example, when a sample is cooled to a liquid nitrogen temperature without magnetic field (zero field cooling : ZFC) and then a

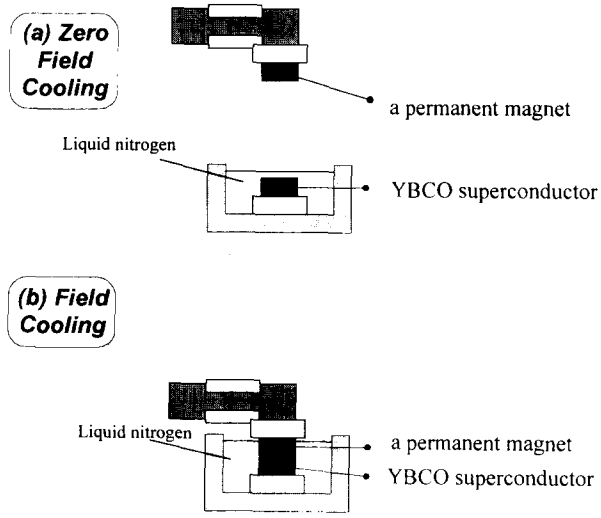

Fig. 5. Schematic of (a) zero field cooling and field cooling methods.

permanent magnet is approach to the superconductor, the external field is mostly rejected from the superconductor. In contrast, when the superconductor is cooled to 77 K in the magnetic field of the permanent magnet (field cooling : FC), a lot of the external magnetic field is trapped inside the superconductor. To know the interaction of the field trapped in the superconductors to the external magnetic field, we measured the force-distance curves of the YBCO superconductors cooled either by ZFC and FC methods (see Fig. 5).

2. 3. Polarity change of a permanent magnet

In order to know the interaction of the trapped field and the polarity of the external field, we examined the force-distance curve versus the variation of the polarity of the permanent magnet. For this work, the single-domain YBCO sample was cooled either by ZFC and FC methods, then a permanent magnet was moved toward and away from the sample and then the force-distance curve is measured. After the first test, the polarity of the permanent magnet was changed to an opposite sign and then the force-distance measurement test was done again for the same samples, as schematically shown in Fig. 6.

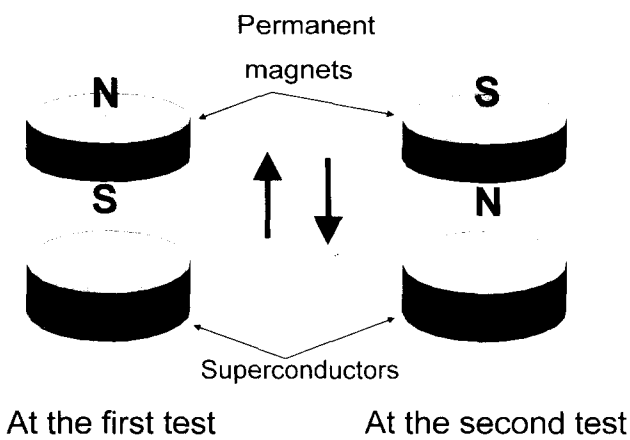

Fig. 6. Schematic of the polarity changing experiment.

3. Results and discussion

3. 1. Levitation force of the multi-domain sample

Figure 7 shows force-distance curve of multi-domain YBCO sample cooled by ZFC (open circles) and FC method (closed circles). The sample was annealed at 500 ℃ for 40 h in flowing oxygen after melt texturing heat treatment. As a permanent magnet was moved toward and away from the ZFC and the FC samples, it showed a hysteresis behavior. Such a hysteresis curve was reported to be due to the flux pinning[1]. Repulsive forces of the ZFC sample at 10 mm and at 1 mm distances are 0.8 kgf and 3.5 kgf, respectively. The maximum attractive force of 0.25 kgf is achieved at 15 mm gap. To know the effect of a test turn on the hysteresis behavior, the test was repeatedly performed for the same sample. All the hysteresis curves were the same as the first one. This implies that the amount of the magnetic fields trapped in the superconductor were almost same regardless of a test turn.

The force-distance curve of the FC sample also shows a hysteresis curve but the mode is different from that of the ZFC sample. As the permanent magnet was moved away from the sample, the maximum attractive force is 1.5 kgf at the 0.25 mm gap but at the second

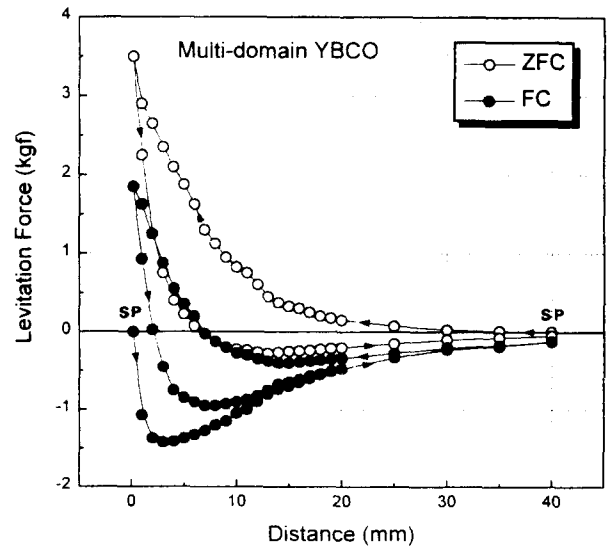

Fig. 7. Force-distance curves of the multi-domain YBCO sample zero-field cooled(open circles) and field cooled(closed circles). SP denotes a starting point.

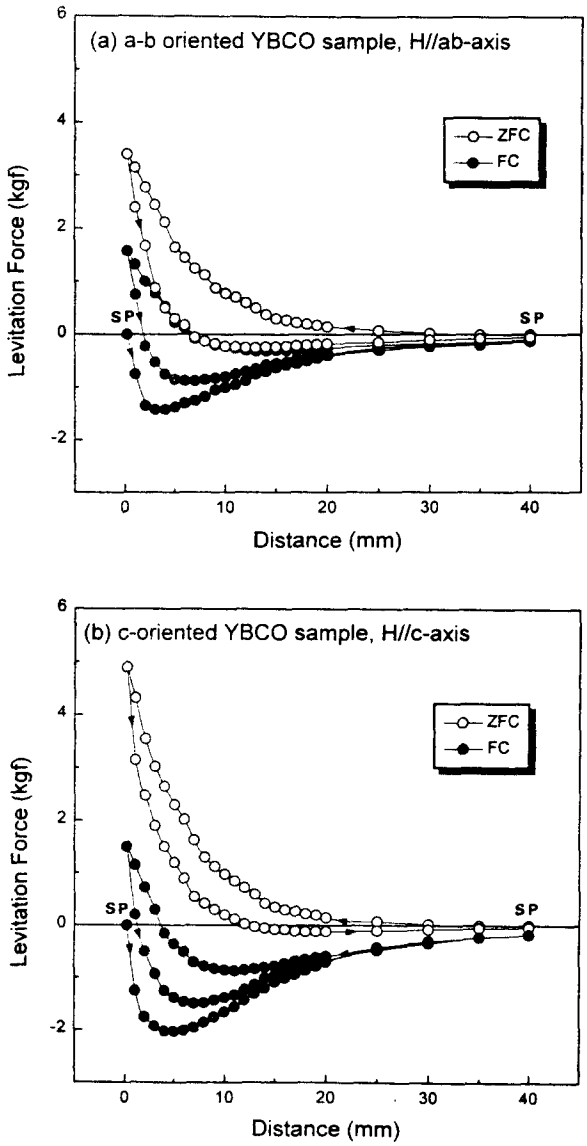

Fig. 8. Force-distance curves of the single-domain YBCO samples grown to (a) ab-axis and (b) c-axis. SP denotes a starting point.

test it is reduced to 1 kgf at 8 mm gap. The maximum repulsive is about 2 Kgf, which is smaller than that of the ZFC sample. The test was also done repeatedly for the same sample. All the force-distance curves were the same as the second one.

3. 2. Levitation force of the single-domain samples

Figure 8 shows force-distance curve of the single-domain YBCO sample grown to (a) ab-axis (H//a-b axis) and (b) c-axis (H//c-axis), cooled either by ZFC or FC method. As can be seen in Fig. 7 (a), the force-distance curves of the sample grown to the ab-axis are similar to those of the multi-domain sample of Fig. 7. The maximum repulsive and attractive forces of the ZFC sample are 3.5 kgf and 0.25 kgf, respectively, which are similar values to those of the multi-domain YBCO, in spite of the larger grain size of the sample than that of the multi-domain sample. This indicates that the rejection of the external field for H//a-b is not strong. In the case of the ZF sample, the repulsive (1. 6 kgf) and the attractive force (1 kgf) are smaller than those of the multi-domain YBCO sample.

On the other hand, as can be seen Fig. 8 (b), the repulsive force of the ZFC sample grown to the c-axis is as large as 5 kgf while the attractive force is as small as 0.1 kgf. This indicates that the rejection of the external field for H//c-axis is much stronger that for H//a-b. The repulsive and the attractive forces of the FC sample are 1.5 kgf and 2.0 kgf, which are larger than those of the sample grown to the ab-axis. Referring to our previous result[18], the magnetization was a function of the crystal orientation of a Y123 crystal. The magnetization (M) for H//c-axis is several times as large as that for H//ab-axis. The large levitation force of the sample grown to the c-axis is seems to be attributed to the large magnetization for H//c-axis.

3. 3. Trapped magnetic field in the multi- and single-domain sample

The magnetic field trapped in the ZFC and FC samples after the force-distance measurement was measured by using of a hole probe. Figure 9 shows the distribution of the trapped magnetic field at the centerline of (a) multi-domain and (b) single-domain YBCO samples (H//c-axis). As can be seen in Fig. 9 (a), the trapped magnetic field of the multi-domain sample is asymmetric. This is due to the presence of several domains in the sample. It can be seen that the trapped magnetic field in the FC sample is larger than that of the ZFC sample. The maximum trapped magnetic field of the ZFC and the FC samples are 550 G and 750 G, respectively.

On the other hand, the field distribution of the single-domain sample (H//c-axis), shows a symmetric mode. Compared to the multi-domain sample, larger magnetic field is trapped in the single-domain sample. Only one peak point is present at the center of the FC sample. Meanwhile, the amount of the trapped magnetic field of the ZFC sample is small and the distribution is almost flat. This implies that the ZFC sample strongly rejects the external magnetic field. The maximum magnetic field trapped in the FC sample is 1800 G, which is three times as large as that (600 G) of the ZFC sample. This is comparable to that of the multi-domain sample that showed 35% difference in trapped magnetic field be-

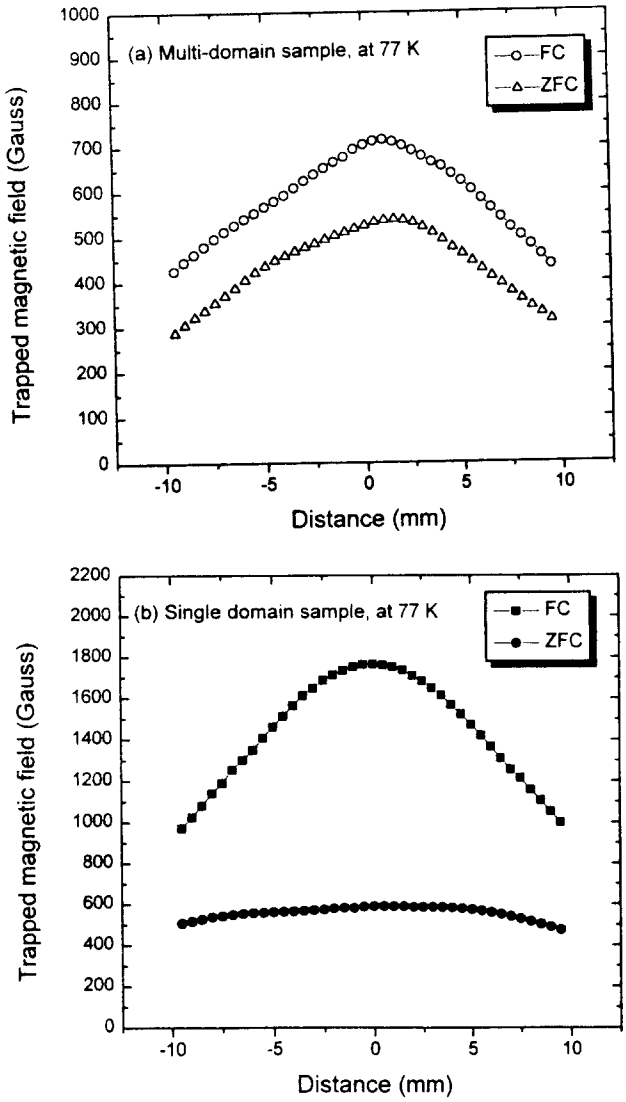

Fig. 9. Trapped magnetic field of (a) multi-domain and (b) single-domain YBCO samples zero-field cooled and field cooled.

tween the FC and the ZFC samples.

The variation of the repulsive and the attractive force of the ZFC and the FC samples of single and multi-domain can be explained by the difference of the magnetic field trapped in the samples. As the superconductor is cooled to 77 K in the field of the permanent magnet, the magnetic field penetrates the whole sample that is in a normal state. Then, when the sample reaches a superconducting state by cooling, much of the penetrated magnetic field is trapped inside the sample. If the polarity of the external magnetic field is positive, the sign of the magnetic field trapped at the top of the superconductor is negative. The interaction between the external magnetic field and the trapped field makes an attractive force between the superconductor and the permanent magnet. The more magnetic fields are trapped, the larger attractive force is formed.

On the other hand, when a sample is cooled without magnetic field, there is no trapped field in the sample. As a permanent magnet moves toward the sample, most of the external field was rejected while some is trapped. The amount of the magnetic fields trapped or rejected will depend on the cooling method as well as the J_c and the grain size of the superconductor, i. e., the size of the magnetic shielding current radius (r) of eq. (3). Owing to the smaller trapped magnetic field and stronger rejection of the external field in the ZFC, the smaller attractive and the larger repulsive forces form in the ZFC sample, compared to the FC sample. In addition to this, r of the single-domain sample is larger than that of the multi-domain sample. The magnetization (M) for H//c-axis is larger than that for H//ab-axis. These are the reasons why the levitation force of single and multi-domain samples varied with the cooling method and the crystal orientation.

3. 4. Variation of a levitation force by changing of a polarity of a permanent magnet

We investigated the effect of the polarity change of the permanent magnet on the levitation force of single-domain sample (H//c-axis). Figure 10 shows the force-distance curves of the ZFC sample (open circles) at the first test and the variation (closed circles) when the test was done again after the polarity was changed. As can be seen in figure, the variation of the force-distance curve is small when changing the polarity from S to N. The increase of the repulsive force is less than 10 %. In the ZFC sample, the trapped field of an opposite sign to the external magnetic field is very small due to the

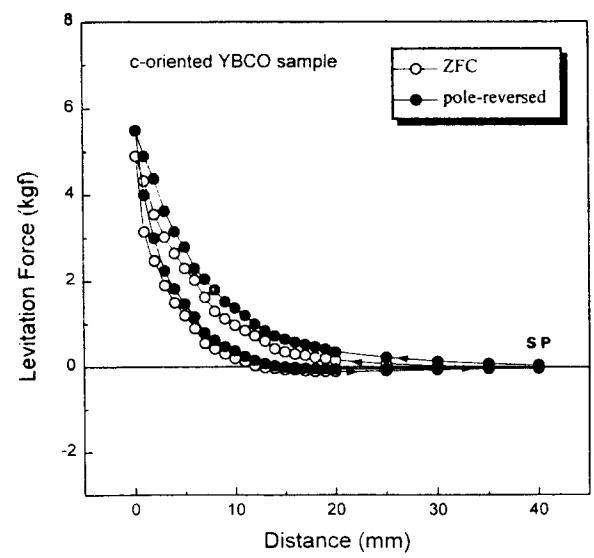

Fig. 10. Variation of force-distance curve of the ZFC sample (single domain) after polarity change of a permanent magnet. SP denotes a starting point.

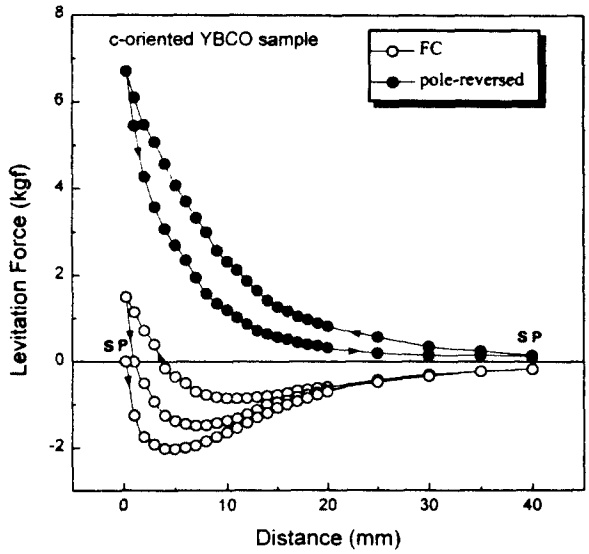

Fig. 11. Variation of force-distance curve of the FC sample YBCO(single domain) after polarity change of a permanent magnet.

strong rejection. As the polarity of the permanent magnet was changed, the sign of the trapped magnetic field is the same as that of the external field. Then, it produces an additional repulsive force due to the interaction between two components of the same polarity.

Figure 11 shows the variation of the force-distance curve of the FC sample vs polarity change. Unlike the result of the ZFC sample, the force-distance curve of the second test shows remarkable increase of repulsive force and decrease of an attractive force. The repulsive and the attractive forces of the ZFC sample at the first test is 2 kgf and 1.50 kgf, respectively but they are changed to 7 kgf and 0 kgf at the second test. The large variation of the force-distance curve is also attributed to the interaction between the trapped magnetic field and the external field. In the FC sample, a lot of magnetic fields are trapped. It appears as a large attractive force term in the first test. Then, when the polarity of the permanent magnet is changed to an opposite sign and the test is done again, the trapped magnetic field interacts with the external magnetic field of the same sign. It produces large repulsion between two components.

3. 5. Levitation force vs sample thickness

The thickness dependence of the levitation force of the single domain YBCO sample was examined for (H// c-axis). Figure 12 shows the repulsive force versus sample thickness estimated from force-distance curves of the ZFC samples. Initial sample thickness of the sample was 14 mm. After every force-distance tests, the

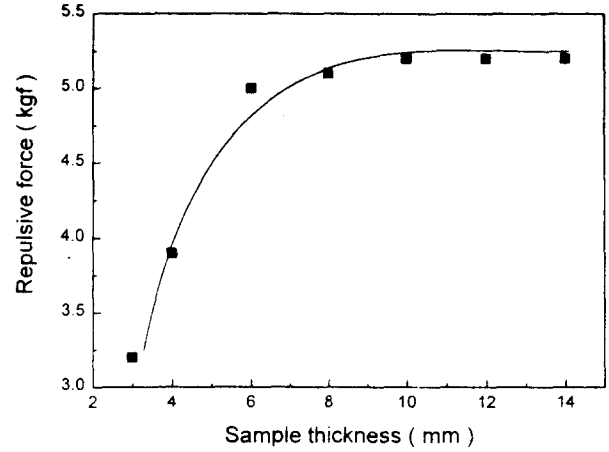

Fig. 12. Thickness dependence of levitation force of the ZFC sample of single domain (H//c-axis).

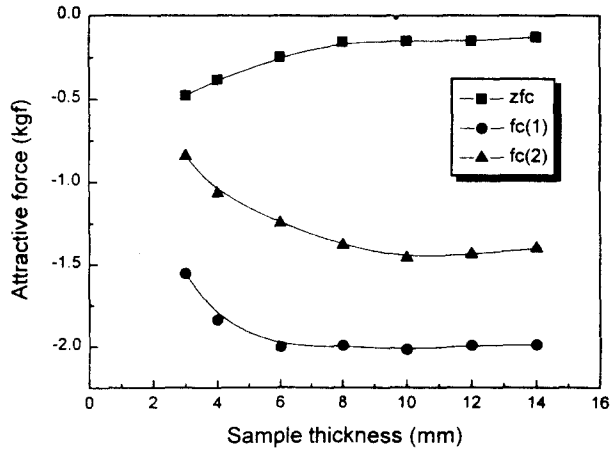

Fig. 13. Thickness dependence of the attractive force estimated of H//c-axis of the ZFC and FC samples of single domain. The closed circles(fc(1)) and the closed triangles(fc(2)) was estimated from the first force-distance test of as-cooled sample and from the second force-distance test, respectively.

bottom of the sample was ground with SiC papers to reduce sample thickness. As can be seen in figure, the maximum repulsive force of the sample is 5 kgf and is almost constant in the thickness ranges from 14 mm down to 8 mm. Below 8 mm thickness, however, the levitation force is remarkably reduced; at 4 mm and 3 mm thickness, the levitation force is 3.8 kgf and 3.2 kgf, respectively.

Figure 13 shows the thickness dependence of the attractive force estimated of H//c-axis of the ZFC and FC samples of single domain. The attractive force has a negative sign in the force-distance hysteresis curve. The closed circles (fc(1)) and the closed triangles (fc (2)) were estimated from the force-distance curve of as-cooled sample (the first force-distance test) and from the second force-distance curve, respectively. The attractive forces of the ZFC sample are less than 0.5

kgf. This is because the ZFC sample strongly rejects the external field and hence the trapped magnetic field in the sample is small while that of the FC sample shows the opposite behavior. Interestingly, the attractive force of the ZFC sample decreases with increasing sample thickness. It is not easy to clearly explain the reason why the attractive force of the ZFC sample decreased with decreasing sample thickness. Probably, some of the external field penetrates the whole sample and then trapped in the sample, because the thickness is thin enough. It might produce more attractive force compared to the samples of lager thickness. On the other hand, the attractive force of the ZFC sample shows the thickness dependence similar to that of the repulsive force of Fig. 12. It increases with increasing sample thickness up to 6 mm. Above 6 mm thickness, the attractive force are nearly constant. Since many magnetic fields are trapped in the FC sample, the attractive forces are larger than those of the ZFC samples. At the first test, the maximum attractive force at the first and the second test is 2.0 kgf and 1.4 kgf, respectively.

The relationship between levitation force of type II superconductor and sample thickness was expressed by following equation[19],

$$F = 4R^3MH_{c1}L/3Z^2 \quad (4)$$

Where R is radius of a permanent magnet, M is magnetic moment of a permanent magnet, H_{c1} is critical magnetic field of a superconductor, L is a thickness of a superconductor and Z is a distance between a superconductor and a permanent magnet. This equation assumed that the external magnetic field penetrates the whole sample thickness. According to this equation, the levitation force of the superconductor has a linear dependency on the sample thickness. Wang et. al measured the levitation force of the sinter-forged YBCO samples of different thickness and they found that it increased linearly up to 5 mm thickness and then reached a constant value in the thickness range from 5 mm to 8 mm[20]. Murakami et. al also reported the thickness dependence of the levitation force of the melt-powder-melt growth processed YBCO (multi-domain)[21]. Referring to their result, the levitation force increased linearly up to 10 mm thickness and was not linear in the range from 10 to 20 mm thickness[21]. The result of this study is well consistent with these results. However, the values of the thickness that correspond to the saturation point were different each other. This may be due to the fact that the penetration depths of a magnetic field in the samples was different each other, since it is dependent on the grain size J_c and the external magnetic field. In the case of the single crystalline YBCO with high J_c, the penetration depth of the external magnetic field would be smaller than that of the meltprocessed multi-domain and the poly-grain sample of small grain size.

5. Conclusions

Variables affecting the magnetic levitation force of the melt-textured YBCO superconductors have been studied. The levitation force was significantly dependent on the factors of the cooling method, the crystal orientation and sample thickness of the superconductors and the polarity of the used permanent magnet. To achieve large attractive force, field cooling is better than zero field cooling. In contrast, the larger repulsive force is achieved in the zero field-cooled sample. This is practically important, because the capacity and the stability of a levitation rotor depend on the amount of the repulsive and the attractive force. The repulsive force single domain sample grown to the c-axis (H//c-axis) is much larger than those of the sample grown to the a-b direction (H//ab-axis). The repulsive and the attractive forces have thickness dependence. It increased with increasing sample thickness and then reached the saturation point. The results of the polarity change of the permanent magnet were very informative in understanding the interaction between the trapped magnetic field and the external field.

Acknowledgment

This work was financially supported by the Ministry of Science and Technology (MOST), Korea.

References

1. F. C. Moon, M. M. Yanoviak, R. Ware, Appl. Phys. Lett. **52** 1534 (1988)
2. E. H. Brandt, Appl. Phys. Lett. **53** 1554 (1988)
3. M. Murakami, T. Oyama, H. Fujimoto, T. Taguchi, S. Gotoh, Y. Shiohara, N. Koshizuka and S. Tanaka, Japan J. Appl. Phys. **29** L1991 (1990)
4. C. K. McMichael, K. B. Ma, M. W. Lin, M. A. Lamb, R. L. Meng, Y. Y. Xue, P. H. Hor and W. K. Chu, Appl. Phys. Lett. **59** 2442 (1991)
5. C. Gabrys, J. R. Hull and T. M. Mulcahy, Am. J. Phys. **60** 1153 (1992)
6. W. K. Chu, K. B. Ma, C. K. McMichael and M. A. Lamb, Appl. Supercond. **1** 1259 (1993)
7. F. C. Moon and P-Z. Chang, Appl. Phys. Lett. **56**

397 (1990)
8. J. R. Hull, T. M. Mulcathy, K. L. Uherka, R. A. Erck and R. G. Abboud, Appl. Supercond. **2** 449 (1994)
9. H. J. Bornemann, C. Urban, P. Boegler, T. Ritter, O. Zaitsev, K. Weber and H. Rietschel, Physica C **235-240** 3455 (1994)
10. S. Nakamura, ISTEC Journal **1** 43 (1993)
11. M. Murakami, Appl. Supercond. **1** 1157 (1993)
12. M. Murakami, Melt processed high-temperature superconductors (Singarpore: World Scientific) p 127 (1992)
13. M. Daeumling, J. M. Seuntjens and D. C. Larbalestier, Nature (London) **346** 332 (1990)
14. B. Martinez, F. Sandiumenge, S. Pinol, N. Vilalta, J. Fontcuberta and X. Obrados, Appl. Phys. Lett. **66** 773 (1995)
15. H. Teshima, M. Morita and M. Hashimoto, **269** 15 (1996)
16. C-J. Kim, K-B. Kim, I-S. Chang, D-Y. Won, H-C. Moon, D-S. Suhr, J. Mater. Res. **8** 699 (1993)
17. C-J. Kim, H-W. Park, K-B. Kim and G-W.Hong, Supercond. Sci. Technol. **8** 652 (1995)
18. C-J. Kim and P-J. McGinn, Physica C **222** 177 (1994)
19. F. Hellman, E. M. Gyorgy, D. W. Johnson Jr., H. M. O'Bryan and R. C. Scherwood J. Appl. Phys. **63** 447 (1988)
20. J. Wang, M. M. Yanoviak and R. Raj, Am. Ceram. Soc. **72** 846 (1989)
21. M. Murakami, Melt processed high-temperature superconductors (Singarpore: World Scientific) p 322 (1992)